

Interstratified Clays. I. Theoretical

RODNEY TETTENHORST,

*Department of Geology and Mineralogy, The Ohio State University,
Columbus, Ohio 43210*

AND RALPH E. GRIM

*Department of Geology, University of Illinois,
Urbana, Illinois 61801*

Abstract

A method for computing the diffraction effects from interlayered clay minerals is formulated, and the results are compared with those obtained using MacEwan's method. The method allows examination of individual layer transforms or of the mean for any given set and can calculate effects not readily obtained with MacEwan's method, *e.g.*, three-component systems. Results from both methods are in good agreement. Differences in the results were caused by the particular composition distribution assumed for either method. Positions and shapes of diffraction maxima are determined by composition, composition distribution, the presence of one-layer spacings, and the distribution of the d values, in addition to the kind of interlayering. The kind of interlayering between I , a 10 Å repeat layer, and M , a 17 Å repeat layer, *e.g.*, random or ordered, is most readily determined in the mid-composition range, that is, approximately $0.75 < p_M < 0.25$. The concept of *IMII* superlattice units formulated by Reynolds and Hower (1970) is reinterpreted. Patterns interpreted as due to *IMII* ordering can be explained by the existence of a montmorillonite layer deeply imbedded within an otherwise normal 10 Å crystallite. The latter interpretation may give some insight into differences between clay minerals termed illite and K-bentonites having similar expandable character.

Introduction

Most analyses of interstratified clays in recent years have utilized or have been based on the method formulated by MacEwan and co-workers (1956, 1958, 1959, 1961). Reynolds and Hower (1970; hereafter designated R&H) have extended the methods of MacEwan to computer analysis and have matched calculated and experimental diffraction patterns for a variety of cases. The favorable agreement for the majority of the comparisons reinforces one's belief in the corrections of the MacEwan approach. Certain of the conclusions of R&H, however, seem suspect. For example, they conclude that (a) virtually all illite/montmorillonites are ordered for $p_m \leq 0.40$, and (b) a special kind of ordering is present for $p_m \leq 0.10$. These conclusions raise questions such as: (1) Why should ordering be restricted to a particular structure/composition range? (2) How do these conclusions explain the nature of substances such as the type illite from Fithian and related clay minerals (Gau-

dette, Eades, and Grim, 1966)? (3) How do these conclusions fit with the "frayed-edge" concept of Bray (1937) and, more recently, of others? (4) What is the role played by the component having a single glycol layer sandwiched between two silicate layers? The search for answers to these and other questions led to the investigation of a method alternative to that of MacEwan for computing the X-ray diffraction effects from interstratified clay systems. Natural clays were analyzed, and laboratory experiments were performed which have a bearing on the conclusions of R&H; these are reported in Part II.

The main objective of this paper is to present this alternative computational method, to illustrate the results obtained by using it, and to compare it with the method and results obtained by using MacEwan's methods. Basically, the present study used the Fourier transform methods of Lipson and Taylor (1957), first applied to layer silicates by Ross (1968). Only the one-dimensional diffraction effects of the basal reflections of layer silicates were considered.

The essential correctness of the results obtained by using MacEwan's methods is undoubted. However, it seemed desirable to explore a different method, if only to substantiate and verify what was already known. There are instances, however, in which MacEwan's methods are not applicable or are difficult to apply. For example, the extension of his methods to an analysis of clay systems containing three or more types of layers, with precise attention paid to the incorporation of the scattering effects by the individuals, is a formidable problem even for the computer. Further, MacEwan's method assumes that certain "consistency relations" (1956, p. 97) are obeyed. These relations do not hold for individual cases. The method used herein has the capability of circumventing these difficulties in the MacEwan approach, but it too has some inherent difficulties. Therefore, a secondary objective of this paper is to analyze and compare the results obtained from both methods. The equally important problem of the genesis of the mixed-layer clays or their thermodynamic status (Zen, 1962, 1967) was not considered.

Definitions and Symbols

The terminology and symbols used by MacEwan are adhered to herein. However, some definitions are desirable. N : the number of silicate layers per crystallite. NI : equals $N-1$, the number of interlayer regions or spacings. The identity of individual interlayer spacings is given by letters such as A and B or I and M . I : a 10 Å repeat unit or, more precisely, a unit containing no ethylene glycol layers. M : a 17 Å unit equivalent to montmorillonite or a unit containing two glycol layers. *Component*: a general term covering A , B , etc. *Layer configuration or Case*: a specific arrangement of A , B , and C , e.g., $AAABBAC$ equivalent to an "X-ray particle" or "crystallite." n_A , etc: the number of A layers in a given layer configuration. p_A , etc: the percentage of A in all of the cases under consideration, i.e., the overall proportion of A in the sample. AA , etc: the number of A contacts in a given layer configuration.

MacEwan's Method

The previously referenced papers fully describe MacEwan's method so we shall simply point out those features appropriate for comparison with our method of analysis. The MacEwan method is not designed to compute the diffraction effects of a particular layer configuration. Rather, once p_A , N ,

and p_{AA} are chosen, assuming a two-component interstratification, the coefficients of each term in his series are fixed. Each of the terms corresponds to a particular interlayer spacing, and the coefficients correspond to the relative frequency of the particular spacing. A necessary consequence of this treatment and of the assumption that the "consistency relations" are valid is to superimpose a *particular* distribution of chemical compositions on the crystallites. To make this clear the coefficients used in MacEwan's series are listed in Table 1 for $NI = 3$, $p_A = 0.7$ for random ($p_{AA} = 0.7$) and ordered ($p_{BB} = 0$) interlayering. Looking at the random case, it can be seen that BBB is given a weight or coefficient of 0.027 which implies that "crystallites" composed solely of B occur with a probability of 0.027. Further, multiplying each of the coefficients, e.g., ABB , by the corresponding percentage of B in that particular term, i.e., 0.67, then summing, the overall proportion of $B = 0.3$ is obtained. In other words, a particular "distribution of chemical compositions" is assumed to be present.

Similarly, the MacEwan coefficients are set forth in Table 1 for regular interlayering. The "composition distribution" here is more restricted about the mean overall composition than for the random case. This is necessary since BB contacts are forbidden. The data in Table 1 further show that for a spacing represented by $2B$'s and $1A$, a larger probability is accorded to the array having B on the ends, i.e., AAB and BAA , rather than ABA . This is a consequence of the "consistency relations." However, it is conceivable that clays may occur in nature that have B 's "on the inside" only. MacEwan's method would not correctly represent such a situation. Similar analyses extended to other p_A values

TABLE 1. MacEwan's Coefficients for $NI = 3$ for $p_A = 0.7$, and $p_B = 0.3$ for Random ($p_{BB} = 0.3$) and Regular Interlayering ($p_{BB} = 0$)

Term	p(Random)	p(Regular)
AAA	0.343	0.22857
AAB	.147	.17143
ABA	.147	.30
BAA	.147	.17143
ABB	.063	0.0
BAB	.063	.12857
BBA	.063	0.0
BBB	.027	0.0

enable one to demonstrate that the distribution of compositions is wider and generally has smaller coefficients for overall compositions in the mid-range, say $p_A \sim 0.5$, and is narrower and has generally larger coefficients for large values of p_A (or p_B), e.g., $p_A = 0.9$. The distribution of compositions for regular interlayering is always more restricted about the mean than that of the corresponding random case, i.e., for a given p_A . These observations are true irrespective of NI . In short, the MacEwan method tacitly assumes the existence of crystallites having a particular "composition distribution" once p_A and p_{AA} are fixed. However, given a single N , e.g., $N = 11$, for all crystallites in a given sample, then arbitrarily setting $p_A = 0.8$, one can envision a situation in which all crystallites have "identical compositions," i.e., $8A$ and $2B$. Although highly restricted, this "narrow composition distribution," i.e., all crystallites have a composition equivalent to the overall mean composition of the sample, may better approximate a given clay.

Along the same lines, the presumption that the kind of interlayering is specified by a knowledge of a single term such as p_{AA} is a necessary consequence of the consistency relations. The existence of a single layer configuration with a given n_A is thereby precluded. With the MacEwan method it may not be possible to distinguish between specific configurations such as $AABAAABAAA$ and $ABAAABAAAA$, whereas, in fact, these two layer configurations give distinct transforms. The reason for this is the spread of compositions inherent in the MacEwan calculation. A fixed arrangement of B 's and A 's and sharply restricted values of n_A in all of the crystallites may more accurately describe some real clays. In such instances the consistency relations of MacEwan are not valid and the clay cannot be adequately described by any values of p_{AA} , etc. It seems likely that it is this feature inherent in the MacEwan method that led R&H to devise an artifice, i.e., an *IMII* superlattice unit, which circumvents the MacEwan coefficients and in effect changes the composition distribution and also restricts the positions of the components within the crystallites. This extension of the MacEwan method may not be warranted since it leads to a conclusion of doubtful validity. We will show later that a different interpretation of "Kalkberg-type" diffraction patterns is possible.

Let us pursue the foregoing from a different viewpoint and examine the conclusion of R&H that

virtually all illite/montmorillonite interlayered mixtures are ordered for $p_M \leq 0.4$. Employing the MacEwan method in the way they did means that the kind of interlayering can be specified by knowing any one of the probability coefficients p_{AA} , etc. Assuming a two-component system and $p_A > p_B$ one can examine p_{AA} as a function of p_A for the kinds of interstratification, mechanical ($p_{AA} = 1$), random ($p_{AA} = p_A$), and regular [$p_{BB} = 0$, therefore $p_{AA} = (p_A - p_B)/p_A$]. This examination leads to the conclusion that the p_{AA} values are most different and, therefore, the kind of interlayering is easiest to specify, in the mid-composition range. For all practical purposes the p_{AA} values for ordered and random interlayering are identical for $p_A \sim 0.9$ and they are similar even for $p_A = 0.8$. Real clays may differ not only in the kind of interlayering but also in size distribution of the crystallites, chemical composition and composition distribution, distribution of d values, or in structural details such as inverted tetrahedra. These differences can act to reduce the distinction between clays resulting from different kinds of mixing. On the basis of this analysis it would appear that the kind of interstratification is most readily determined only in the mid-composition range, e.g., $0.75 < p_A < 0.25$.

Method of Analysis

A computer program¹ was written for $CuK\alpha$ radiation to calculate the squared modulus of the layer transform in the c^* direction for interstratified clay systems containing up to three components. All calculations included contributions from both real and imaginary terms. The resulting diagrams allow a comparison of various hypothetical mixed-layer clays whose sole differences are structural/compositional. The calculations are free of any additional assumptions concerning the pertinent L_p factor, crystallite size distribution, or apparatus functions. They do not represent "complete diffraction patterns" such as those given by R&H. G^2 was computed as a function of θ . The d values shown above prominent maxima on the diagrams were determined to the nearest $0.05^\circ 2\theta$, this being the approximate precision with which one can read real diffraction diagrams for a goniometer scanning speed of $1^\circ 2\theta/\text{minute}$ and a chart speed of 30 inches/hour. Com-

¹ For a copy of this program, order document AM-75-002 from the Business Office, Mineralogical Society of America, suite 1000 lower level, 1909 K Street, N.W., Washington, D. C. 20006. Please remit \$1.00 for the microfiche.

putations were made for the two-component illite/montmorillonite (10 Å/17 Å) system and covered the entire composition range. As the study progressed and the utility of the method became apparent, the effect of (a) the one-glycol layer complex and (b) composition distribution was investigated. Each transform was calculated with the origin taken at the plane of the octahedrally coordinated atoms in an end silicate layer. A montmorillonite unit was defined as a two-glycol layer interlamellar space, and an illite as an interlamellar space containing no glycol molecules. The scattering factors and other parameters used (Table 2) were quite similar to those used by R&H so as to facilitate comparison with their work. The same silicate layer was used for all components.

The detailed nature of the one-glycol layer complex has not been fully investigated. The parameters chosen to represent this component are in agreement with the scanty literature on the subject (Bradley *et al.*, 1958; Brunton, Tettenhorst, and Beck, 1963) and the premise that it was similar to the 17 Å component.

Transforms for particular layer configurations were generated one at a time for a given NI and component array, *e.g.*, $NI = 5$ and $IIIMI$, for which in this example $p_M = 0.2$. In addition all possible arrangements of $4I$'s and $1M$ were generated and a "mean" pattern calculated. An obvious advantage of this approach is that individual transforms can be examined. Potential disadvantages are (a) the composition of each crystallite is restricted to being identical with the overall composition, and (b) calculations are made for a single NI . The former is easily overcome while the latter is not. Consequently, calculations were made for $NI = 5$, $NI = 10$, and $NI = 20$ to determine the effect of thickness. The reason for choosing these NI values was that a preliminary laboratory study showed that many natural illite/montmorillonites dehydrated for 1 day at 400°C give apparent NI values in this range as determined from the measured breadths of the diffraction maximum at about $27^\circ 2\theta$ with $CuK\alpha$ (see Tettenhorst and Roberson, 1973, for details.) This procedure limits the particular compositions that can be investigated once NI is fixed; *i.e.*, p_M can vary only in 0.20 increments for $NI = 5$, only in 0.10 increments for $NI = 10$, *etc.* Generation of all possible individual transforms and computation of a mean transform is simple if NI is small, say $NI = 5$, since the number of layer configurations is

TABLE 2. Structural Data Used for the Computation of Interstratified Clay Patterns

Atom	Z(Å)*	P	B(Å ²)
The "end" layer			
Potassium	-5.00	0.3	1.68
Oxygen	-3.27	3.0	1.68
Silicon	-2.70	2.0	1.68
Oxygen	-1.06	3.0	1.68
Aluminum	0.0	1.0	1.68
The 10Å layer			
Aluminum	0.0	1.0	1.68
Oxygen	1.06	3.0	1.68
Silicon	2.70	2.0	1.68
Oxygen	3.27	3.0	1.68
Potassium	5.00	0.8	1.68
Oxygen	6.73	3.0	1.68
Silicon	7.30	2.0	1.68
Oxygen	8.94	3.0	1.68
Aluminum	10.00	1.0	1.68
The 17Å layer			
Aluminum	0.0	1.00	1.68
Oxygen	1.06	3.00	1.68
Silicon	2.70	2.00	1.68
Oxygen	3.27	3.00	1.68
Glycol (CH ₂ OH)	6.12	0.85	11.00
Glycol	7.07	0.85	11.00
Water	7.94	0.40	1.68
Potassium	8.50	0.40	1.68
Water	9.06	0.40	1.68
Glycol	9.93	0.85	11.00
Glycol	10.88	0.85	11.00
Oxygen	13.73	3.00	1.68
Silicon	14.30	2.00	1.68
Oxygen	15.94	3.00	1.68
Aluminum	17.00	1.00	1.68
The 13.5Å layer			
Aluminum	0.0	1.00	1.68
Oxygen	1.06	3.00	1.68
Silicon	2.70	2.00	1.68
Oxygen	3.27	3.00	1.68
Potassium	5.27	0.30	1.68
Glycol	6.27	0.75	11.00
Glycol	7.23	0.75	11.00
Potassium	8.23	0.30	1.68
Oxygen	10.23	3.00	1.68
Silicon	10.80	2.00	1.68
Oxygen	12.44	3.00	1.68
Aluminum	13.50	1.00	1.68

*Atomic coordinates of the opposite "end" layer were equal to
 $+Z + (17 \cdot n_M + 10 \cdot n_I + 13.5 \cdot n_{13.5})$

given by $(NI)/(n_A!n_B!)$. For $NI = 10$ and $n_A = 9$ ($p_A = 0.9$), ten arrays are possible, and only half of these need be calculated to produce a mean since identical transforms are generated by configurations that are symmetrical. For $NI = 10$ the number

of possible cases increases to 210 in the mid-composition region, for $p_A = 0.6$. For $NI = 20$ the number of cases is quite large at any composition, and it is simply impractical to compute so many individual cases in order to arrive at a mean transform. The power of the MacEwan method is that all such cases are considered with the additional advantage that p_A can be chosen equal to any value and not restricted to a composition such that $p_A = n_A/NI$.

A specific example will be given to show how the computation of thousands of cases was circumvented. There are 38,760 ways of arranging 14A's and 6B's for $NI = 20$ ($p_A = 0.7$). Some experimentation showed that the mean transform calculated from 100 randomly selected cases produced a reasonable approximation to the true mean. This was checked in two ways. First, a second batch of 100 cases randomly selected as before was generated, and the resultant mean transform was virtually identical to the first. This process was repeated for several p_A values with identical results. Further, these mean patterns compared very favorably with those calculated for the same p_A value for $NI = 10$, for which all possible cases could be calculated.

One cannot be certain that just any batch of 100 randomly selected layer configurations will provide a reasonably accurate mean transform. To ensure a reasonable agreement, the individual cases in sets of 25 were examined for AA and BB contacts and 4 such sets were put together to form the 100 to produce the "correct number" of AA and BB contacts. The "correct number" of AA contacts is given by the relation $x_{AA} = p_A \times N_C \times (n_A - 1)$ for which N_C is the number of layer configurations (here = 100) and $(n_A - 1)$ is the maximum number of AA contacts. The procedure is identical for the BB contacts. The reader may better understand this relationship with a simple example: Assume $NI = 5$ and $p_A = 0.6$, for which the total $N_C = 10$. Therefore, $x_{AA} = 12$ and $x_{BB} = 4$, as the reader can easily verify by listing all ten cases.

The procedure described was not necessary to compute a mean transform for a set of ordered configurations since these were always relatively small in number and all could be computed. Ordered is here taken to mean $BB = 0$ and $AA = \text{minimum}$ for $p_A > p_B$. In certain instances, however, mean transforms from a set of "partially ordered" patterns were calculated from a set of 100

individual cases, partial order being defined as $BB = 0$. To take an example, for $NI = 20$, and 12A-8B there are 1280 cases with $BB = 0$. Each of the 1280 cases was assigned a number, and 100 of these were selected randomly for the purpose of computing a mean transform.

Discussion of Results

Two Components

Representative patterns generated by the method described in the previous section are shown in Figures 1-4. Only those in the range $p_M \leq 0.4$ are included herein. Most of the transforms shown are for $NI = 10$; a few computed for $NI = 20$ are included for comparison. "Diffraction ripples" are present on all of these diagrams and are particularly pronounced at low 2θ angles. MacEwan and Ruiz Amil (1959) noted that these diffraction ripples can be attenuated to produce a "smooth curve" by including a distribution of crystallite thicknesses, *i.e.*, several N values are used in the computations. As will be shown later, "smoothing" was also accomplished here by including a distribution of crystallites having different chemical compositions. Although real clays likely represent a distribution in crystallite thickness and composition, their inclusion into the computations constitutes a guess on the part of the investigator as to the true situation.

Any particular pattern shown in Figures 1-4 represents the mean transform calculated for a number of crystallites all of which have the same NI and p_M . For example, the curve shown at the bottom of Figure 2a is the mean of the 45 separate cases which have 8I and 2M layers, *i.e.*, the 45 ways of arranging 8I and 2M layers. Nine of the

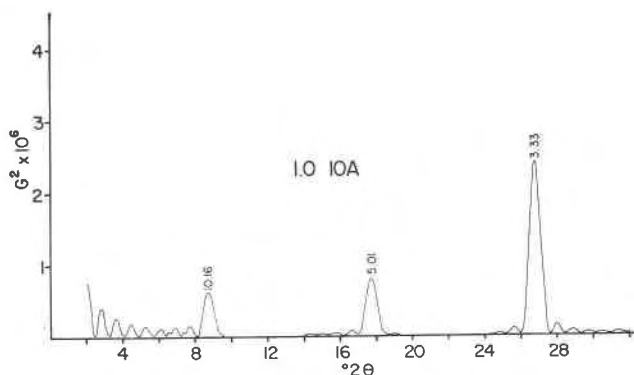


FIG. 1. Calculated diffraction pattern, $p_I = 1.0$, $NI = 10$.

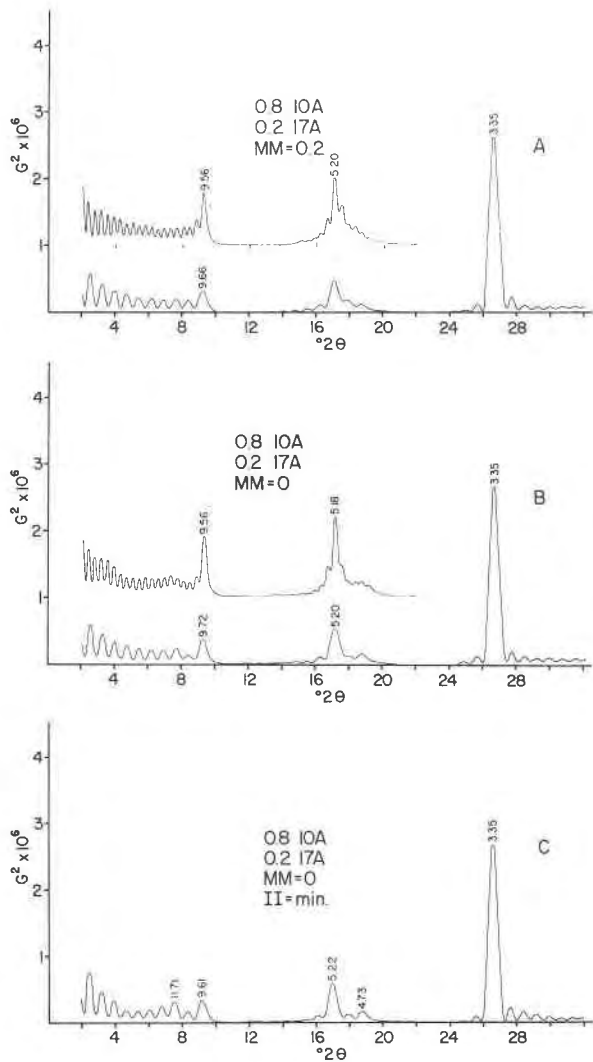


FIG. 2. Calculated diffraction patterns, $p_I = 0.8$. (a) $MM = 0.2$, top $NI = 20$, bottom $NI = 10$; (b) $MM = 0$, top $NI = 20$, bottom $NI = 10$; (c) $MM = 0$, $II = \text{minimum}$, $NI = 10$.

45 cases have touching MM layers, a proportion exactly equal to the overall percentage of M in the "sample," *i.e.*, $MM = 0.2$. This "mean" transform appears to give a diagram strictly analogous to MacEwan's "random" situation and will be so considered in the rest of this paper. Also shown are the mean transforms calculated for "fully ordered" situations, *i.e.*, $MM = 0$ and II contacts are minimum. For example, the curve in Figure 2c represents the mean of 21 cases in which the M layers are separated from each other and likewise the I layers. This "fully separated" mean transform appears analogous to MacEwan's "ordered" situation.

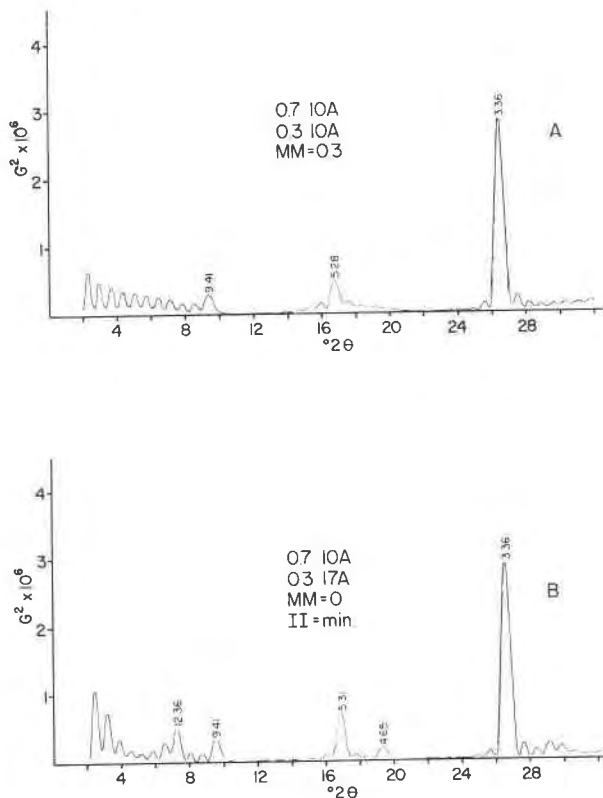


FIG. 3. Calculated diffraction patterns, $p_I = 0.7$, $NI = 10$; (a) $MM = 0.3$, (b) $MM = 0$, $II = \text{minimum}$.

The term "separated" appears preferable to "ordered" as it is more descriptive in those instances not in the mid-composition region $p_M \sim p_I$. The essential difference between those mean transforms computed with fully separated cases, *e.g.*, Figure 2c, and those calculated only with the condition that $MM = 0$, *e.g.*, Figure 2b, is that the latter contain some layer configurations having M 's on the ends of the crystallites.

Interlayering Defined

The kinds of interlayering as used in this study are defined in Table 3 in terms of Q values. The Q values are, for a representative set of layer configurations, the proportion of contacts of a given kind, say AA , compared to the maximum number of contacts of that type that would occur if all cases were completely segregated. The Q values given in the table are valid only for $p_A > p_B$ and $NI \geq 3$. The expression for Q_{AA} (separated) was obtained from its equivalent $(n_A - n_B - 1)/(n_A - 1)$, the numerator of which denotes the minimum number of AA contacts and the denominator the maximum

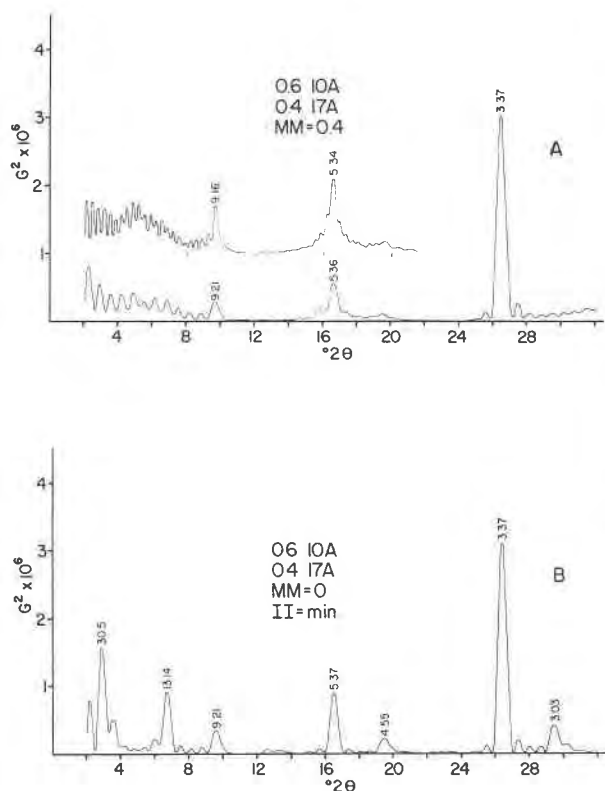


FIG. 4. Calculated diffraction patterns, $p_I = 0.6$; (a) $MM = 0.4$, top $NI = 20$, bottom $NI = 10$, (b) $MM = 0$, $II = \text{minimum}$.

number of AA contacts for a given composition using relations such as $p_A = n_A / (n_A + n_B) = n_A / NI$. Drawn in Figure 5a are continuous curves of Q_{AA} vs p_A for several NI for ordered interlayering and the relation for random. A similar diagram was given by Gilkes and Hodson, 1971. As concluded previously when considering MacEwan's method, the distinction between ordered and random is best determined in the mid-composition range. This point is made clearer in Figure 5b where a conservative

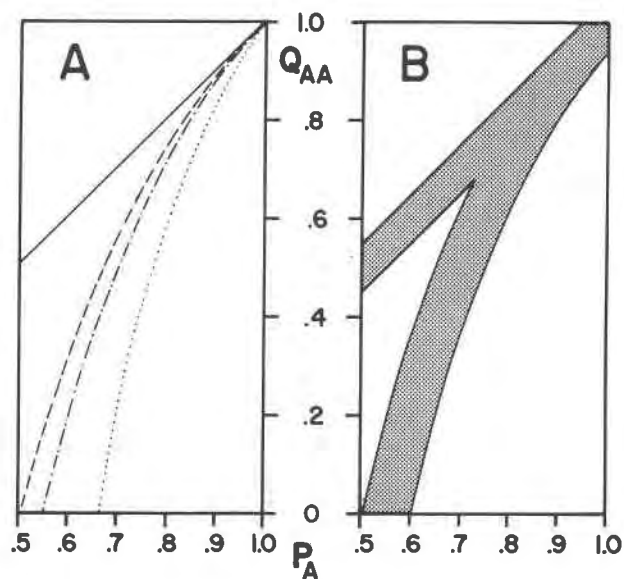


FIG. 5. The proportion of A contacts for random and ordered mixing relative to the maximum number of A contacts if all cases were segregated vs p_A . (a) Random given by ———, ordered $NI = 3$ given by ······, ordered $NI = 10$ given by —·—·—, ordered $NI = \infty$ given by - - - - -. (b) Random and ordered ($NI = 10$) are redrawn assuming p_A known to ± 5 percent.

uncertainty in the value of p_A of ± 5 percent has been applied to both the random and the $NI = 10$ (separated) curves. The overlap of the two regions is severe at $p_A > 0.85$ but not at $p_A = 0.75$. Figure 5a further suggests that the distinction of random and ordered interlayering should be easier for small NI since the curve for the $NI = 3$ separated case is the farthest from the random case. This relationship is not likely to be borne out in practice because of lower intensity and broader maxima with smaller N .

Segregated interlayering as defined in Table 3 is not strictly equivalent to MacEwan's definition of mechanical mixing of individual crystallites. The latter implies individual crystallites while the former means segregation within a crystallite for which one contact exists between the two components. The computed transforms for either are quite similar, however.

Some Observations

The average transforms generated herein for either random or ordered interlayering can be compared with those produced by using MacEwan's method (R&H) in a general way, particularly with

TABLE 3. Definition of the Kinds of Interstratification as Employed in This Study*

Kind of interlayering	Q_{AA}	Q_{BB}	Q_{AB} (or Q_{BA})
Segregated	1	1	1
Mean (Random)	p_A	p_B	$p_A \cdot p_B \cdot NI$
Separated (Ordered)	$\frac{2 \cdot NI \cdot p_A - NI - 1}{NI \cdot p_A - 1}$	0	$p_B \cdot NI$

*Q values for $p_A > p_B$ and $NI \geq 3$

respect to the shape and 2θ position of prominent maxima. Comparison of intensity or diffracted energy is less reliable because the diagrams here lack certain of the factors assumed by R&H, as described earlier. Overall, the same basic information is obtained from either method. In general, the 2θ positions calculated agree well with those cited by R&H in their Table 3. The differences that do occur are confined to the low ($<10^\circ 2\theta$) region (e.g., $9.6^\circ 2\theta$ vs $9.43^\circ 2\theta$ for R&H for $p_m = 0.4$ and $MM = 0.4$). These differences are almost entirely a result of the restricted composition used here versus the distribution inherent in the MacEwan method. This observation suggests that "peak positions" alone cannot be used to determine the percentages of the various components in a natural mixed-layer clay with a very high degree of precision (say to within several percent) since the distribution of chemical compositions of the individual crystallites in real clays is not known.

Hower and Mowatt (1966) attributed the steep rise in the background intensity at low angles ($<4^\circ 2\theta$) to signify the presence of interstratification (p. 847, their Fig. 8). Comparing 0.5μ sized particles of muscovite and illite, as segregated by sedimentation methods, they noted that illite had a steeper background rise, and a broader (001) peak with d slightly greater than 10\AA . The distinctive features of the illite were attributed to interstratification and, specifically, not to "particle size." The present work does not support this conclusion as shown in the figures since the rate at which the background intensity rises at low angles is similar for all diagrams for a given N . Contrary to Hower and Mowatt (1966), the distinctive features of their X-ray pattern of illite compared to muscovite can be attributed primarily to smaller mean crystallite thickness. Identical sedimentation-size-fractions of different layer silicates do not insure that identical crystallite thicknesses will be obtained for both materials (Tettenhorst and Roberson, 1973) nor that the morphological particle thicknesses will be the same since the particles in different samples may vary in their areal dimensions, specific gravity, extent of association with water molecules, etc. Along the same lines R&H have attached considerable significance to the match up of the rise in background at low angles for their calculated and experimental patterns. Their computed patterns contained the powder Lp factor. It is suggested that, if an experimental pattern is encountered whose background

rise cannot be explained by N , then attention should be given to the precise form of the Lp factor. It is possible that not all layer silicates or oriented interstratified clays behave like "powders" but that some may approximate a single crystal in scattering efficiency. MacEwan, Ruiz Amil and Brown (1961) drew a similar conclusion.

Layer Location within a Particle

Shown in Figure 6 are the five individual transforms and their mean, calculated for $NI = 10$ and $9I - 1M$, i.e., $p_M = 0.1$. As the position of the single M layer changes from the "outside of the crystallite" (position 1, Fig. 6a), to the "middle of the crystallite" (position 5, Fig. 6e), the diffraction pattern changes as follows: (a) the maximum at $8.8^\circ 2\theta$, which is rather skewed to low angles, splits into two sharper maxima one of which migrates to $9.0^\circ 2\theta$ and the other develops at about $8.0^\circ 2\theta$; (b) the maximum at $17.6^\circ 2\theta$ splits into two maxima of which the more prominent migrates to $17.2^\circ 2\theta$, the other to about $18.4^\circ 2\theta$. Note that the patterns in Figures 6d and 6e resemble the Kalkberg pattern of R&H (their Fig. 2, p. 30). Possibly a variation of thickness and, perhaps, of chemical composition

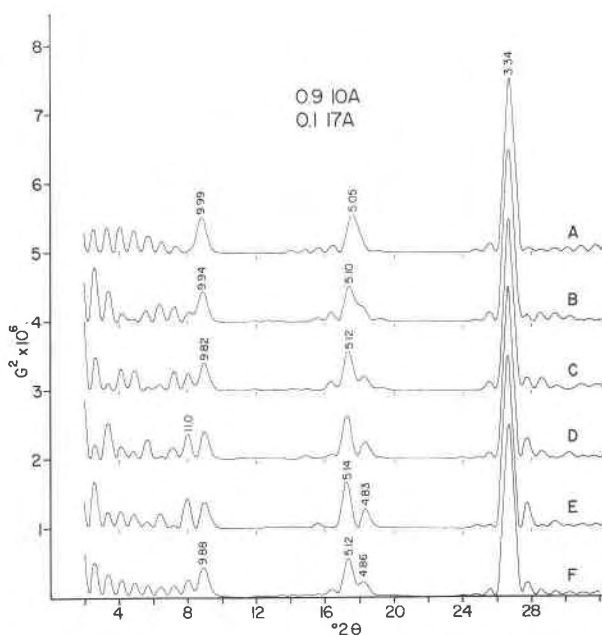


FIG. 6. Calculated diffraction patterns, $p_M = 0.9$, $NI = 10$; (a) M in position 1, (b) M in position 2, (c) M in position 3, (d) M in position 4, (e) M in position 5, (f) mean of (a)-(e).

for the crystallites would give a "smooth" computed pattern that would match very well the experimental pattern of Kalkberg. It is concluded that patterns like the Kalkberg clay—rather than illustrating a special kind of ordering such as *IMII* at a composition, *i.e.*, $p_M \sim 0.1$, where the kinds of interlayering are virtually impossible to distinguish—actually show that M layers are imbedded within the crystallites. Although the conclusion of R&H that Kalkberg-type patterns represent a special kind of ordering may be incorrect, their assignment of the quantity of expanded layers, *i.e.*, $p_M \sim 0.1$, in these interstratified clays appears to be reasonable.

Illites that give X-ray patterns such as Fithian or Grundite (Gaudette, Eades, and Grim, 1966) and the Strasburg "metabentonite" (API No. 37) are common. Glycolated patterns typically show an asymmetrical *001* peak at $10 + \text{\AA}$, this being skewed to low angles, and a rather broad *002* peak at about $17.6^\circ 2\theta$. How are such clays to be interpreted? The presence of some expandable layers is indicated, but the disposition of these expanded layers must be different from that in Kalkberg-type clays. Although speculative it is suggested that the patterns of Fithian-type clays resemble that shown in Figure 6a and, therefore, the crystallites in Fithian may, more than not, terminate on expanded layers. The expanded layers would then define the limit or thickness of those crystallites. This suggestion is in broad agreement with the "core-rind" or "frayed-edge" hypothesis advanced for the structure of these clays by Gaudette, Grim, and Metzger (1966) on the basis of the sorption behavior of cesium. To carry this suggestion one step further, this interpretation might suggest that Fithian-type clays generally represent the effect of "degradation," *i.e.*, the "opening-up" of the particles at their edges or "surfaces" while Kalkberg-type patterns generally represent the effects of "aggradation," the "closing-up" of the particles until the last remaining expandable layer is buried inside the individual crystallites.

Highly-Expandable Clays

Although not shown in the figures, two observations are noted concerning the patterns at the highly expandable end of the *I/M* scale, *i.e.*, $p_M \sim 1.0$. First, compared with the patterns computed for $p_M = 1.0$, the introduction of 10 percent collapsed layers decreases the peak intensity of *001* to about half its value, its position being rather unaffected,

and decreases the position of *002* by about $0.10^\circ 2\theta$. Second, the effect of a layer of glycol molecules on the surfaces or ends of the particles was calculated and compared with the "no-surface-glycol" situation (Tettenhorst and Reynolds, 1971) for both $p_M = 1.0$ and $p_M = 0.9$. The significant effects for both compositions compared to no-surface-glycol were (a) the intensity of the *001* peak decreased about 15 percent and the intensity of *002* increased by 15 percent and (b) the position of *002* increased about $0.1^\circ 2\theta$. Tettenhorst and Roberson (1973) noted that the relative positions of *001* and *002* from a group of montmorillonites were rather scattered and did not fit well with either a surface glycol or no-surface-glycol model. Interstratification was suggested as being responsible for the poor fit and this seems borne out by the present observations. Indeed, it may be difficult to decide from the diffraction patterns of individual montmorillonites what the relative contributions are between surface glycol or a small percentage of non-expanded layers. The transforms shown in this paper and those provided by R&H were calculated assuming no surface glycol.

Composition Distribution

The transforms discussed previously were the mean of some given number of layer configurations for which each individual layer configuration had the same composition. This is not necessary. The method used herein is capable of simulating any composition distribution, in particular, that used in the MacEwan method. The details for one such simulation are set forth in Table 4 for $p_M = 0.2$, $MM = 0.2$, and the resulting mean transform is shown in Figure 8a. The total number of layer configurations used to compute the mean transforms in these instances was 100. The MacEwan coefficient (column 2 in Table 4) was computed for a particular *NI* (= 10) and p_M . This figure determined the number of layer configurations having a given composition, *e.g.*, $7I - 3M$, that were included in the computation of the mean, *i.e.*, 20 cases out of a possible 120. The specific cases used for calculating the mean were selected randomly. A final check was made to insure that the proper number of *II*, *etc* contacts was obtained for the 100 cases before performing the calculation. Several such mean transforms simulating MacEwan's composition distribution were computed in this manner for various mean p_M values (Figures 7-9). The effect of ordering was also taken into account; two such

TABLE 4. Cases Used to Simulate the MacEwan Composition Distribution for $NI = 10$, $p_M = 0.2$, and $MM = 0.2$

Sequence	MacEwan Probability Coefficient	Number of cases
10I	0.107	11
9I - 1M	.268	27
8I - 2M	.302	30
7I - 3M	.201	20
6I - 4M	.088	9
5I - 5M	.026	3
Sum = 0.992		100

patterns for $p_M = 0.2$ are shown in Figures 8b and 8c.

Compared with the transforms shown previously, the most obvious difference is the smoothness of the curves and relative lack of diffraction ripples, except at angles below about $4^\circ 2\theta$. The smoothness is the result of the composition distribution and consequent variety of thickness for $NI = 10$. A comparison of these with their equivalents computed by the MacEwan method shown in R&H indicates a close match of peak positions and peak shapes. Differences in the three transforms illustrated in Figure 8 for $p_M = 0.2$ are discernible, particularly the buildup of scattering at about $7^\circ 2\theta$ for the fully separated case. The presence of a peak in this 2θ region along with a peak between $9-10^\circ 2\theta$ may be an indication of ordering as noted by Reynolds (1967). However, the form and position of peaks in this 2θ range are also very susceptible to composition distribution as noted, and the presence

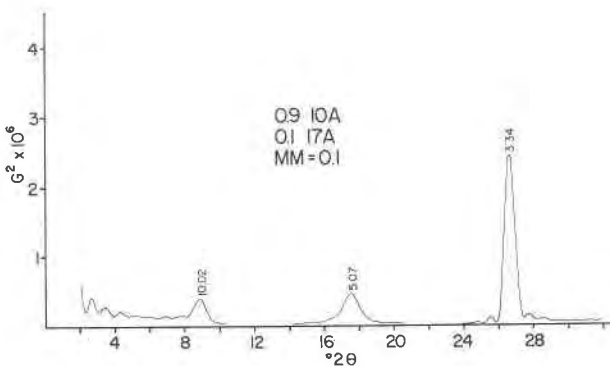


FIG. 7. Calculated diffraction pattern for $p_I = 0.9$, $MM = 0.1$, $NI = 10$, simulating MacEwan's composition distribution.

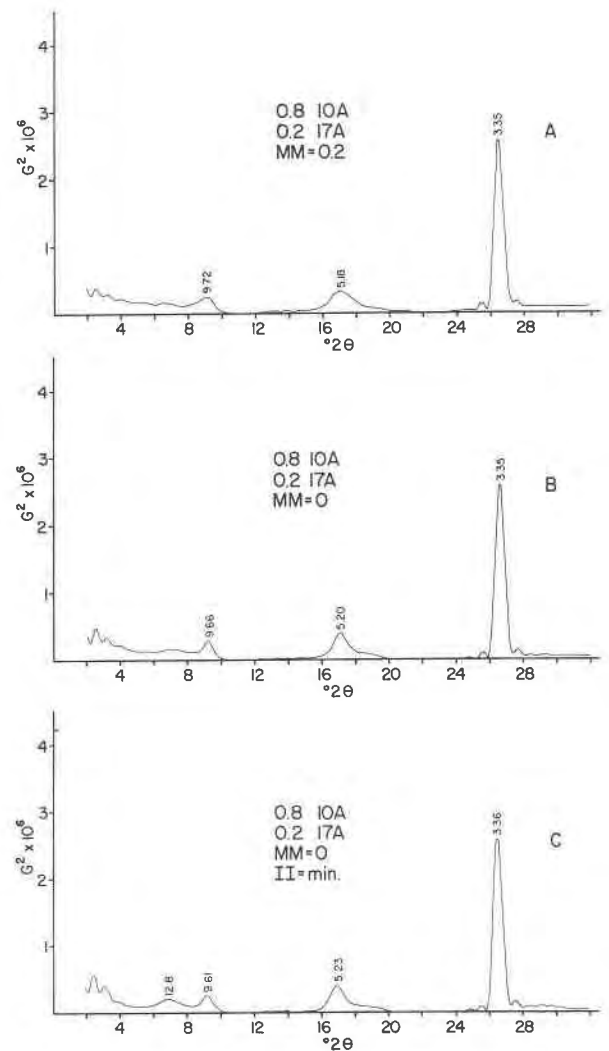


FIG. 8. Calculated diffraction patterns for $p_I = 0.8$, $NI = 10$, simulating MacEwan's composition distribution; (a) $MM = 0.2$, (b) $MM = 0$, (c) $MM = 0$, $II = \text{minimum}$.

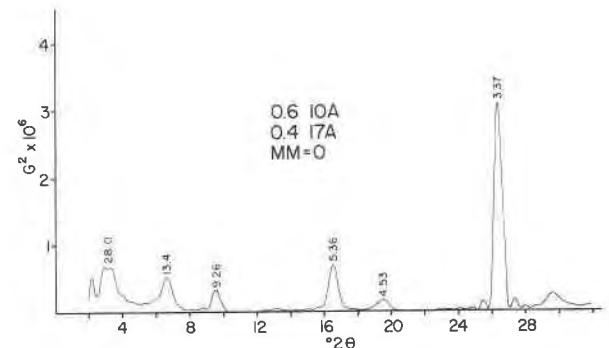


FIG. 9. Calculated diffraction pattern for $p_I = 0.6$, $MM = 0$, $NI = 10$, simulating MacEwan's composition distribution.

of one-layer spacings or d value distributions, as will be shown in Part II.

A notable feature shown in Figures 4b and 9 for ordered or partly ordered cases is the prominent superlattice peak that develops at about $3^\circ 2\theta$ for compositions given approximately by $0.35 \leq p_M \leq 0.65$. Its presence seems to be the surest indication of ordering, as might be expected. When this superlattice peak is indistinct or represented merely by a shoulder or break in the steep background rise at low 2θ , the composition is given approximately by $p_M = 0.30 - .35$. For example, see the X-ray pattern of A.P.I. No. 42 from High Bridge, Kentucky, shown in Figure 4 of Hower, 1967.

Acknowledgments

Appreciation is extended to The Ohio State University Computer Center for granting time and facilities, and to Professor Charles E. Corbató for his advice, particularly with respect to the utilization of a program to generate random numbers.

References

- BRADLEY, W. F., R. A. ROWLAND, E. J. WEISS, AND C. E. WEAVER (1958) Temperature stabilities of montmorillonite- and vermiculite-glycol complexes. *Clays Clay Minerals*, **5**, 348-355.
- BRAY, R. H. (1937) Chemical and physical changes in soil colloids with advancing development in Illinois soils. *Soil Sci.* **43**, 1-14.
- BRUNTON, GEORGE, R. TETTENHORST, AND C. W. BECK (1963) Montmorillonite-polyalcohol complexes: Part II. *Clays Clay Minerals*, **11**, 105-116.
- GAUDETTE, H. E., J. L. EADES, AND R. E. GRIM (1966) The nature of illite. *Clays Clay Minerals*, **13**, 33-48.
- , R. E. GRIM, AND C. F. METZGER (1966) Illite: A model based on the sorption behavior of cesium. *Am. Mineral.* **51**, 1649-1656.
- GILKES, R. J., AND F. HODSON (1971) Two mixed-layer mica-montmorillonite minerals from sedimentary rocks. *Clay Minerals*, **9**, 125-137.
- HOWER, JOHN (1967) Order of mixed-layering in illite/montmorillonites. *Clays Clay Minerals*, **15**, 63-74.
- , AND THOMAS C. MOWATT (1966) The mineralogy of illites and mixed-layer illite/montmorillonites. *Am. Mineral.* **51**, 825-854.
- LIPSON, H., AND C. A. TAYLOR (1957) *Fourier Transforms and X-Ray Diffraction*. G. Bell and Sons, London.
- MACEWAN, D. M. C. (1956) Fourier transform methods for studying scattering from lamellar systems, I. A direct method for analysing interstratified mixtures. *Kolloid Z.* **149**, 96-108.
- (1958) Fourier transform methods for studying x-ray scattering from lamellar systems, II. The calculation of x-ray diffraction effects for various types of interstratification. *Kolloid Z.* **156**, 61-67.
- , AND A. RUIZ AMIL (1959) Fourier transform methods for studying x-ray scattering from lamellar systems, III. Some calculated diffraction effects of practical importance in clay mineral studies. *Kolloid Z.* **162**, 93-100.
- , AND G. BROWN (1961) Interstratified clay minerals, Chapter XI in *X-ray Identification and Crystal Structures of Clay Minerals*, Ed. G. Brown, Mineralogical Society, London.
- REYNOLDS, R. C. (1967) Interstratified clay systems: Calculation of the total one-dimensional diffraction function. *Am. Mineral.* **52**, 661-672.
- , AND JOHN HOWER (1970) The nature of interlayering in mixed-layer illite-montmorillonites. *Clays Clay Minerals*, **18**, 25-36.
- ROSS, M. (1968) X-ray diffraction effects by non-ideal crystals of biotite, muscovite, montmorillonite, mixed-layer clays, graphite and periclase. *Z. Kristallogr.* **126**, 80-97.
- TETTENHORST, RODNEY, AND R. C. REYNOLDS (1971) Choice of origin and its effect on calculated X-ray spacings for thin montmorillonite crystals. *Am. Mineral.* **56**, 1477-1480.
- , AND HERMAN E. ROBERSON (1973) X-ray diffraction aspects of montmorillonites. *Am. Mineral.* **58**, 73-80.
- ZEN, E-AN (1962) Problem of the thermodynamic status of the mixed-layer minerals. *Geochim. Cosmochim. Acta*, **26**, 1055-1067.
- (1967) Mixed-layer minerals as one-dimensional crystals. *Am. Mineral.* **52**, 635-660.

Manuscript received, April 19, 1974; accepted for publication, July 17, 1974.